HHS Public Access

Author manuscript

Biopolymers. Author manuscript; available in PMC 2017 February 24.

Published in final edited form as:

Biopolymers. 2009 January ; 91(1): 52–60. doi:10.1002/bip.21081.

Circular Dichroism and UV-Resonance Raman Investigation of the Temperature Dependence of the Conformations of Linear and Cyclic Elastin

Zeeshan Ahmed, **Jonathan Scaffidi**, and **Sanford A. Asher***

Department of Chemistry, University of Pittsburgh, PA 15260

Abstract

We used electronic circular dichroism (CD) and UV resonance Raman (UVRR) spectroscopy at 204 nm excitation to examine the temperature dependence of conformational changes in cyclic and linear elastin peptides. We utilize CD spectroscopy to study global conformation changes in elastin peptides, while UVRR is utilized to probe the local conformation and hydrogen bonding of Val and Pro peptide bonds. Our results indicate that at 20 °C cyclic elastin predominantly populates distorted β-strand, β-type II and β-type III turn conformations. At 60 °C, the β-type II turn population increases while the distorted β-strand population decreases. Linear elastin predominantly adopts distorted β-strand and β-type III turn conformations with some β-type II turn population at 20 °C. Increasing temperature to 60 °C, results in a small increase in the turn population.

Keywords

Elastin; UV-Resonance Raman Spectroscopy; circular dichroism; inverse temperature transition; β-turns; distorted β-strand

INTRODUCTION

In recent years the unique elasticity and resilience of elastin based peptides has drawn interest from both the biophysics and material science communities.[1–16] Elastin is an important structural peptide that enables elastic deformations of biological assemblies. Biological motion, for example, is enabled by elastin's unique ability to repetitively and reversibly deform upon stress. We each benefit from the elastic properties of elastin, where, hopefully, our aorta reversibly contracts and expands 10^9 times during our lives. Biochemical, genetic and structural analysis of elastin fibers has demonstrated that the elastin found in skin, blood vessel walls and lung tissue is a composite of an amorphous component (elastin) and a microfibrillar component (fibrillin). Elastin mimetic peptide $(VPGXG)_n$-where n is the number of repeat pentamers, is widely used as a model system for studying elastin's remarkable viscoelastic properties.

*To whom correspondence should be addressed. Department of Chemistry, University of Pittsburgh, Pittsburgh, PA 15260 Phone: 412 624 8570 Fax: 412 624 0580 asher@pitt.edu.

Over the years, considerable effort have been expended to elucidate the mechanism of elastin's unique elasticity.[3–13,17–26] The elastic properties are thought to be associated with or a consequence of elastin's unusual phase transition behavior, which closely resembles that of the thermal volume phase transition behavior of poly(*N*-isopropylacryamide) (PNIPAM).[27–39] PNIPAM polymers contain both hydrophilic and hydrophobic regions whose exposure to the aqueous medium may change as the polymer collapses at high temperature. The transition temperature of PNIPAM polymers is determined by a delicate balance between amide-water hydrogen bonding, isopropyl group-water interaction, and van der Waals interactions between the hydrophobic groups.[30]

Elastin exists as a highly mobile expanded chain below a certain characteristic temperature that the elastin literature refers to as the "critical temperature, T_c". Above T_c, the peptide chain adopts a compact conformation resulting in a significantly decreased radius of gyration and reduced chain mobility.[24] The elastin literature calls this thermal behavior an "inverse temperature transition".[20,40] Just as for PNIPAM,[29,30] the transition temperature of elastin peptides can be tuned by changing the hydrophobicity of the polymer. In the $(VPGXG)_n$ system we can substitute at the X residue.[41]

The remarkable viscoelastic properties of elastin peptides are thought to arise from weakening of peptide-water interactions at elevated temperatures which results in a hydrophobic collapse of the peptide[15,24,40] The balance between enthalpy and entropy determines the critical temperature. Below T_c, the favorable enthalpic contribution from amide-water hydrogen bonds and/or charged side chain-water interactions compensate for the unfavorable entropy arising from solvation of hydrophobic groups.[24] The relative importance of this enthalpy advantage is decreased at higher temperatures. Part of this loss results from increased thermal fluctuations which weaken peptide-water hydrogen bonds. The loss of water-peptide hydrogen bonding-derived stabilization, forces the extended peptide chains to contract to minimize the impact of the unfavorable entropy.[24] Increased librational entropy[42–45] of the released water molecules reduces the entropic cost of hydrophobic solvation and compensates for the loss of configuration entropy incurred upon elastin's transition.[3,4,22,23]

Unfortunately, there are no high resolution NMR or X-ray structures of elastin because of the high mobility of the peptide's backbone.[40] This lack of detailed knowledge regarding conformational transitions in elastin has significantly impeded efforts for establishing a clear link between structure and function of elastin peptides. Based on spectroscopic studies, Venkatachalam and Urry[23] proposed that that upon an increase in temperature, the highly mobile peptide chains adopt a rigid, well ordered β-spiral conformation. A β-spiral is composed of repetitive β-type II turns, which form a helix-like structure without inter-turn (i − i + 4) hydrogen bonds.[17,22,23,46] This model is supported by NMR and Raman studies.[47] These spectroscopic studies found that the collapsed state of the polymer resembles the structure of cyclic $(VPGVG)_3$ peptide crystallized from a mixed water/D_2O-methanol solvent.[17,18,22,23]

Below T_c, the cyclic peptide exists in a β-type II turn conformation which at high concentrations precipitates at elevated temperatures, presumably into an ordered β-spiral-

like conformation.[23] Reiersen et al[40] used CD spectroscopy to demonstrate that the transition is independent of chain length. The smallest cooperative unit appears to be the pentamer (VPGXG), indicating that long range interactions do not play a significant role in elastin's inverse transition. The authors demonstrate that small elastin peptides show a broad transition between 1 and 77 °C where the CD global minimum (200 nm) decreases with increasing temperature. The temperature dependent behavior of (VPGVG)-repeat elastin peptides appears to be pH independent.[40]

While Venkatachalam and Urry's β-spiral model is consistent with some of the spectroscopic studies, it does not agree with studies of tissue derived, water-swollen elastin fibers, which indicate that elastin collapses to a random coil-like conformation.[48–51] Recent molecular dynamics simulations by Li et al[3,4] suggest that the collapsed state of elastin is best described as a "compact amorphous structure". The MD study found that when starting from an idealized β-spiral conformation at low temperatures, the expanded peptide chain retained significant β-spiral population. At high temperatures, however, β-turns and β-strand-like conformations dominate. These results suggest that the collapsed state of elastin may be best described as a molten globule where the peptide chain locally adopts a short-range β-spiral-like conformation.[3,4]

In this work we used CD and UVRR to examine temperature-dependent conformation changes in cyclic and linear elastin. Our results indicate that the cyclic peptide predominantly populates distorted β-strand, β-type II and type III turn conformations. In contrast, linear elastin predominantly populates β-type III turn and distorted β-strand conformations, with a minor β-type II turn population, as well.

Experimental

The UV resonance Raman spectrometer has been described in detail elsewhere.[52] Briefly, 2 mW of 204 nm UV light was generated by Raman-shifting the 355 nm 3rd harmonic output of an Nd:YAG laser (Coherent, Infinity) in H_2 gas. These UV pulses were then focused at ~45 degrees from the normal to produce a sub-mm spot near the interior surface of a rotating fused silica NMR tube (Wilmad) filled with ~1 mL of the sample solution. A 135° backscattering geometry was used for collecting the Raman scattered light, which was then dispersed by a custom-made subtractive double monochromator onto a back thinned CCD camera (Princeton Instruments-Spec 10 System).[52]

The 15-residue long cyclic $(VPGVG)_3$ and linear elastin *GVG*$(VPGVG)_2$*VP* were obtained from the Pittsburgh Peptide Synthesis Facility (PPSF, >95% purity) and used at 1 mg/ml concentrations at pH 7. The cyclic peptide was prepared by cyclization of the linear variant (PPSF, >95% purity). Raman spectra (average of three five minute spectra) were normalized relative to the peak height of the 0.1 M perchlorate's 932 cm^{-1} band. Three replicate measurements of separately prepared elastin solutions were recorded to ensure measurement reproducibility. Solution pH was adjusted by adding small aliquots of HCl or NaOH. Temperature dependent CD spectra (average of 10 spectral accumulations) of similarly prepared solutions (pH ~5) at 1 mg/ml were measured on a Jasco-715 spectropolarimeter using a 200 μm path length quartz cell. CD and Raman spectra of linear elastin measured at

20 °C subsequent to the elevated temperature measurements were similar to those measured prior to the temperature increase, indicating the absence of significant photo- or thermal degradation or irreversible aggregation. The CD spectrum of cyclic elastin shows a slight overall decrease in amplitude after heating. This change likely derives from temperature induced degassing/bubble formation on cell walls at high temperatures.

Results and Discussion

Cyclic Elastin

We examined the temperature dependence of cyclic elastin's conformation by measuring the circular dichroism (CD) spectra between 0 and 50 °C (Fig 1). At 0 °C the cyclic elastin spectrum shows a local minimum at ~222 nm, a maximum at ~207 nm and a global minimum below 200 nm. Previous studies indicate that in elastin peptides the presence of a relatively weak minimum at ~222 nm is indicative of the presence of β-type I/III turn conformation, while the maximum at ~207 nm is indicative of a β-type II turn conformation.[24,40,53] It should be noted that typically a minimum at 222 nm is associated with either an α-helix or 3_{10}-helix like conformation. However, in such cases the global minimum is located above 200 nm, typically around 207-205 nm.[53–55] In cyclic elastin the global minimum is located below 200 nm, which indicates a significant random coil population, thus, excluding the possibility that the feature at 222 nm arises from either α-helix or 3_{10} helix-like conformations. These results indicate the global conformation of cyclic elastin contains significant random coil and β type II and β-type III turn conformations. As the solution temperature is increased, the global minimum value becomes less negative (Fig 2). A decreased global minima is regarded as a hallmark of elastin's inverse temperature transition.[24,56,57] No significant changes are observed in either the 222 or 207 nm region (Fig 1).

We further probed the temperature dependence of cyclic elastin's backbone conformation by measuring the 204 nm excited UV resonance Raman spectra at 20 and 60 °C (Fig 3). There are only three unique types of peptide bonds in elastin, those involving Gly, Pro and Val. The Raman amide bands significantly differ for these peptide bonds such that they are easily differentiated.

Proline is a tertiary amide where the pyrrolidine ring side chain loops back onto itself. Consequently, Pro peptide bond lacks the amide hydrogen (NH)[58,59] and all the C-N stretching motion is concentrated in a single Raman band labeled AmII'p (amide II' of proline).[60] The AmII'p band is thought to be sensitive to local conformation and/or hydrogen bonding of the Pro peptide bond.[61–63]

In secondary amino acids such as Val and Gly the amide hydrogen's bending motion (NH_b) couples with the C-N_s and $C_\alpha H_b$ motion, resulting in a complex spectrum that shows multiple bands, namely the AmII (C-N_s with some NH_b at ~1550 cm^{-1}), $C_\alpha H_b$ (1380 cm^{-1}), and various AmIII bands (predominantly C-N_s and NH_b, between ~1200 cm^{-1} and 1280 cm^{-1}).

The Gly peptide bond spectrum spectroscopically differs from other non-prolyl peptide bonds due to its two low mass hydrogen atom side chains. The Gly peptide bonds show a single AmIII band at 1284 cm^{-1} ($AmIII^G$) in the amide III region.[64,65] In contrast the Val peptide bonds show typical Raman spectra in the AmIII region comprising of the $AmIII_1$, and $AmIII_2$ bands along with the conformationally sensitive $AmIII_3$ band. The conformation sensitivity of the $AmIII_3$ band arises due to Ψ angle dependent coupling between NH_b and $C_\alpha H_b$ motions.[66] In extended PPII like conformations the NH and $C_\alpha H$ hydrogens are cis allowing for a maximum coupling between NH_b and $C_\alpha H_b$ motions. However, in α-helical conformations the NH and $C_\alpha H$ hydrogens are trans which results in insignificant coupling.[67] In Gly, this conformation sensitivity may be lost or decreased due to the presence of two C_α hydrogens ($C_\alpha H_2$) which allows for some coupling with $C_\alpha H$ for all accessible Ψ angles.

Thus, for elastin peptides we use the AmII'p and the Val $AmIII_3$ bands to probe the conformation and/or hydrogen bonding state of Pro and Val peptide bonds. We utilize CD spectroscopy along with the UVRR information on the Val and Pro peptide bonds to infer Gly peptide bond conformation.

As shown in Fig 4, we deconvoluted the measured 204 nm excited UVRR spectrum into a sum of a minimum number of mixed Gaussian and Lorentzian bands by using the peak fitting routine in Grams (Galactic Industries Corporation, Grams version 5). The broad ~1660 cm^{-1} AmI band (predominantly C=Os) is composed of two overlapping bands centered at 1674 and 1635 cm^{-1}. Thomas *et. at.* have reported that the amide I region of crystalline cyclic elastin suspended in its mother liquor shows two prominent AmI bands at ~1652 and 1676 cm^{-1}. These authors suggest that both the 1652 and 1676 cm^{-1} AmI bands likely derive from β-type II turn conformations.[47] However, the origin of the frequency difference between these two AmI bands was not discussed.

The two underlying AmI components (1674 and 1635 cm^{-1}) do not result from intrinsically different frequencies for the amide I bands of the Val, Gly and Pro peptide bonds. Polyproline peptides show AmI bands in the region between 1640 cm^{-1} and 1650 cm^{-1}, while polyglycine peptides show AmI bands at ~1650 cm^{-1}.[65,68,69] The typical non-prolyl, non-glycyl peptide bonds in unfolded peptide conformations typically show a single broad amide I band at 1665 cm^{-1}.[70,71] This frequency spread would not typically result in two overlapping AmI bands at 1635 and 1674 cm^{-1}.

The frequency differences observed for the amide I band either results from significantly different amide bond conformations or from different carbonyl hydrogen bonding. Lazarev *et. al.*[68] reported that the IR absorption spectra of Z-$(Gly_1$-Pro_2-$Gly_3)_4$-OMe peptide in D_2O shows a broad AmI band that appears to be composed of three different AmI components located at 1632 cm^{-1}, 1650 cm^{-1} and 1669 cm^{-1}. These authors attributed the high frequency 1669 cm^{-1} AmI component to the dehydrated/weakly hydrogen bonded carbonyl of Gly_3.[68] Recently Spiro and coworkers reported observing a similar high frequency UVRR AmI band in the PPII (1677 cm^{-1}) and β-sheet (1670 cm^{-1}) conformation of polyK peptide.[72] Boury and coworkers[73] suggest that a similar the high frequency AmI component in Gliadin and Globulin proteins derives from random coil and/or β-turn conformations.

Our CD results indicate that the cyclic elastin peptide predominantly adopts an extended β-strand like conformation with some β-turn character, discounting the possibility that the high frequency AmI component derives from β-sheet-like conformations. We therefore, conclude that the broad 1635 cm^{-1} AmI component of elastin likely derives from hydrogen bonded peptide bonds, whereas the 1674 cm^{-1} component of elastin derives from dehydrated or weakly hydrogen bonded peptide bonds.

The peptide bond dehydration may correlate with weak amide-amide hydrogen bonding in β–turn like conformations. X-ray studies of cyclic elastin peptide $(VPGVG)_3$ indicate three β-type II turns. The β-turn spans the VPGV unit and includes a hydrogen bond between the two Val peptide bonds. The other Gly residue appears to serve as a bridge between adjacent turns.[47,74] It is likely that in aqueous solutions, the weakly hydrogen bonded turn conformation is stabilized against strong peptide-water hydrogen bonding by the bulky β-branched side chains of Val which are known to restrict water access to the peptide backbone.[75] A lack of significant change in elastin's AmI region at high temperatures (Fig 2) suggests minimal changes in elastin's hydrogen bonding state. Similar results were reported by Thomas *et al.* who did not observe any significant change in the amide spectra upon the phase transition.[47] A lack of significant change in the AmI region at high temperatures suggests the inverse temperature transition of elastin does not significantly impact the hydrogen bonding state of the peptide backbone.

The AmII band at ~1558 cm^{-1} involves C-N stretching with some N-H bending.[71] The trough in the AmII region (Fig 3) is an artifact from over-subtraction of the interfering molecular oxygen vibration at 1560 cm^{-1}.

The AmII' band of Pro (AmII'p)[60] located at 1466 cm^{-1} is predominantly a C-N stretch which is thought to be sensitive to local conformation and/or hydrogen bonding of Pro's peptide bond. The AmII'p downshifts from 1466 to 1460 cm^{-1} and its band width (FWHM) appears to narrow from 50 cm^{-1} to 47 cm^{-1} as the solution temperature is increased from 20 to 60 °C (Fig 3). We recently demonstrated that the AmII'p band frequency is sensitive to the peptide backbone conformation of proline.[61] The narrowing of the AmII'p band at high temperatures indicates a narrower conformational distribution of the proline peptide bond at 60 °C.

Takeuchi *et al*[62], suggested that the AmII'p frequency depends on the hydrogen bonding state of Pro.[62,76] If that were true then the observed changes in the AmII'p frequency would suggest weakening of amide-water hydrogen bonds at high temperature. However, we see little evidence from the AmI band for peptide bond dehydration.

The $C_\alpha H_b$ band is located at 1385 cm^{-1}. The presence of the resonance enhanced $C_\alpha H_b$ band is correlated with the presence of non α-helical conformations.[70,77] In elastin peptides the $C_\alpha H_b$ intensity derives only from the Val and Gly peptide bonds, although as discussed above, we expect that the impact of Val peptide bond conformational changes on the $C_\alpha H_b$ band intensity would be more than what would occur for the Gly peptide bond.

The Amide III region has recently been examined and reassigned.[78–82] The $AmIII_1$ band is located at 1346 cm^{-1}, while a weak $AmIII_2$ band is located at ~1322 cm^{-1}. In cyclic elastin

these bands derive only from Val peptide bonds. The 1287 cm^{-1} AmIII band likely derives from glycine peptide bonds. The broad $AmIII_3$ band located at ~1246 cm^{-1} is composed of two overlapping bands at ~1251 and ~1233 cm^{-1} (Fig 3) which derive from the Val peptide bonds.

Recently, Mikhonin *et al*[83] quantitatively demonstrated that the $AmIII_3$ band frequency depends upon the ψ dihedral angle and the hydrogen bonding state of the amide bond.[78,83] Furthermore, Mikhonin and Asher[84] demonstrated that the resonance enhanced AmIII and $C_\alpha H_b$ bands each scatter independently i.e. there is negligible coupling between adjacent peptide bonds. The UVRR spectra in the AmIII and $C_\alpha H_b$ region can therefore be regarded as a linear sum of individual peptide bonds. Hence, the $AmIII_3$ spectra represents the time-averaged conformation distribution of the peptide bonds.[54,85]

Using Mikhonin *et al's*[83] methodology for correlating the ψ dihedral angle with the $AmIII_3$ band position, we find that the 1251 cm^{-1} band could originate from either a β-type III turn-like conformation ($\psi \sim -35°$) or a distorted β-strand-like conformation ($\psi \sim +165°$, see table 1). The presence of a strong $C_\alpha H_b$ band indicates the existence of significant non-α-helical conformations. As discussed above, the presence of a minimum at 222 nm along with a global minimum below 200 nm in the CD spectra (Fig 1) indicates that some fraction of cyclic elastin exists in a β-type III turn conformation with a significant content of random-coil like conformation. We therefore conclude that the 1251 cm^{-1} Raman band of cyclic elastin likely contains contributions from both the distorted β-strand and type-III turn like conformations. Similarly, Mikhonin *et al's* data suggest the 1233 cm^{-1} $AmIII_3$ band could originate from either anti-parallel β-sheet ($\psi = +135°$) or β-turn ($\psi = 0°$) conformations. Taking our cue from previous elastin studies[23] we assign the 1233 cm^{-1} $AmIII_3$ band to β-type II turn conformations of the Val peptide bonds.

The spectra in the $C_\alpha H_b$ and $AmIII_3$ region show some changes in band intensities and position as the temperature is increased from 20 to 60 °C. The frequency of $C_\alpha H_b$ band is temperature independent.[54,78,86] The $C_\alpha H_b$ band region in the difference spectrum shows a small positive peak; decrease in the $C_\alpha H_b$ band intensity at high temperatures indicates a decrease in the extended state (distorted β-strand) population (Fig 3). The $AmIII_3$ band appears to show increased band intensity at 60 °C, as indicated by a trough in the difference spectrum at ~1235 cm^{-1}, which suggests an increased β-type II turn population.

Linear Elastin

At 20 °C, the 204 nm UVRR spectrum of linear elastin (Fig. 5A) resembles the 20 °C cyclic elastin spectrum—suggesting that the ensemble conformations of linear elastin's Val and Pro peptide bonds are similar to their counterparts in cyclic elastin. The cyclic and linear elastin peptides have similar sequences, although the cyclic peptide has an extra peptide bond (P-G) due to cyclization of the linear variant.

The CD spectrum shows a smaller β-type II turn population for linear elastin than for cyclic peptide as indicated by a less prominent band maximum at ~207 nm (Fig 5B).[12,24,40] A lack of significant difference in the UVRR spectra of linear elastin versus cyclic elastin suggests

that the increased turn population is localized in conformational changes at the Gly peptide bonds. Previous studies suggested that linear's elastin's Gly residues are highly mobile.[87]

The CD spectra of linear elastin show little temperature dependence at 222 and 207 nm (Fig 6), whereas the global minimum below 200 nm becomes less negative with increasing temperature (Fig 2 and 6). The linear slope of the melting curve indicates a non-cooperative transition (Fig 2). The presence of a local minimum at ~222 nm indicates the presence of β-type III turn conformation, while a weak maximum at ~207 nm is indicative of some β-type II turn conformation.[40] Presence of the global minimum below 200 nm indicates a significant random coil population.[40,53]

The mean residual ellipticity (MRE) of linear elastin at 198 nm of ~ 4000 deg*cm^2*residue^{-1} *dmol^{-1} at 0 °C is significantly smaller than the values reported by Reiersen *et al*.[40] for short elastin-like peptides. Although, the sequence of peptides in the two studies differs (our peptides have extra Val and Pro residues at the N-terminus) both Reiersen *et al*.'s and our study show similar spectral features. The relatively small MRE indicates greater β-turn character[40] for our peptide, which likely arises due to the presence of hydrophobic terminal Val and Pro residues. Our CD results indicate that the linear elastin peptide predominantly populates random coil and β-type III turn-like conformations along with a small population of β-type II turns.

As shown in Fig. 7, spectral deconvolution of the UVRR spectrum of linear elastin at 20 °C reveals a similar AmI region as cyclic elastin's with AmI bands at ~1635 cm^{-1} and 1672 cm^{-1}. The trough in the AmII region is an artifact arising due to over-subtraction of the 1560 cm^{-1} molecular oxygen contribution. The AmII'p is located at 1463 cm^{-1}, while the resonance-enhanced $C_\alpha H_b$[70,77] is located at 1383 cm^{-1}. The AmIII$_1$ band is located at 1348 cm^{-1} while a weak AmIII$_2$ band is located at 1318 cm^{-1}. The AmIII^G is located at ~1285 cm^{-1}. The conformation-sensitive AmIII$_3$ region (deriving from Val) shows a broad band at ~ 1247 cm^{-1} that is likely composed of two overlapping bands located at ~1250 and ~1232 cm^{-1} (Fig 7). According to Mikhonin *et al*.[83] the 1232 cm^{-1} band likely derives from β-type II turn like conformations (ψ ~ 0°), while the 1250 cm^{-1} band likely derives from distorted β-strand (ψ ~ +165°) and β-type III turn-like conformations (ψ ~ −35°, see table 1).

Recently, Ohgo *et al*.[88] utilized solid-state NMR techniques in conjunction with a statistical analysis of Brookhaven Protein Databank (PDB) to estimate the angular distribution of the two central Val peptide bonds (Val 14 and 16) in an isotope-labeled $(VPGVG)_6$ lyophilized peptide. The authors found that Val-14 shows a bimodal distribution of (Φ, Ψ) values at: (−110 ± 20°, 130 ± 20°) and (−75 ± 15°, −15 ± 15°) which constitutes 70% and 30% of total population, respectively. Val-16 residue adopts the (Φ, Ψ) values of (−90 ± 15 °, 120 ± 15°). A bimodal distribution was also observed for the central Gly and Pro peptide bonds suggesting that elastin conformation is an ensemble of multiple conformations with some minor β-spiral contribution. Ohgo *et al*.'s[88] calculated Ψ angle values for Val are similar to our UVRR derived Ψ angles. The slight differences in Ψ angle values likely drive from increased peptide backbone mobility in our aqueous phase experiment. This suggests that that the aqueous conformations observed in our UVRR experiment also occur in the lyophilized solid-state samples of Ohgo *et al*.[88]

As the solution temperature is increased from 20 to 60 °C, the $AmIII_3$ band shows a small increase in band intensity as indicated by a trough in the difference spectrum at ~1237 cm^{-1}, suggesting an increased β-type II turn population (Fig 8). The AmII'p band narrows ($\Delta FWHM = 2\ cm^{-1}$) as the solution temperature is increased from 20 to 60 °C, suggesting a narrower conformation distribution at 60 °C, although the narrowing in linear elastin (($\Delta FWHM = 2\ cm^{-1}$, Fig 8) is just a little less than in cyclic elastin ($\Delta FWHM = 3\ cm^{-1}$, Fig. 2). Furthermore, unlike in cyclic elastin, the band position of the AmII'p band in linear elastin remains invariant with temperature. This suggests that unlike the prolines of cyclic elastin, linear elastin's prolines do not undergo a significant conformation change with increasing temperature.

Conclusion

We utilize electronic circular dichroism (CD) and UV resonance Raman spectroscopy at 204 nm excitation to examine the temperature dependence of conformational changes in cyclic and linear elastin peptides. We use CD spectroscopy to examine global conformation changes in elastin peptides, while UVRR probes the local conformation and hydrogen bonding of Val and Pro peptide bonds. Our results indicate that the cyclic peptide predominantly populates distorted β-strand, β-type II and β-type III turn conformations at 20 °C. At 60 °C, the β-type II turn population increases somewhat while the distorted β-strand population decreases as indicated by changes in the $AmIII_3$ and $C_\alpha H_b$ regions.

The ensemble population of linear elastin is predominantly β-type III turn and distorted β-strand with some β-type II turn population regardless of solution temperature. Increasing temperature results in a small increase in the β-type II turn population; furthermore, we observe narrowing of the AmII'p band with increasing temperature which suggests a narrowed conformation distribution at high temperatures.

Our CD spectra of linear elastin vs. cyclic elastin indicate a greater β-type II turn population for cyclic elastin. However, the UVRR of cyclic and linear elastin do not show any significant differences. This result suggest that the increased type II turn content of cyclic elastin is likely due to cyclization induced conformation changes at Gly peptide bonds.

Our results demonstrate that for both cyclic and linear elastin the global conformation changes are predominantly driven by conformation changes at the proline and glycine peptide bonds, whereas the Val peptide bonds show relatively little conformation changes with increasing temperature. However, the Val peptide bonds are probably not mere spectators; they likely play a pivotal role in the inverse temperature transition of elastin peptides.

We find that both the cyclic and linear elastin peptide show a broad AmI band which is likely composed of two overlapping bands at ~1674 and 1635 cm^{-1}. The 1635 cm^{-1} component derives from hydrogen bonded peptide bonds, whereas the ~1674 cm^{-1} component likely derives from dehydrated/weakly hydrogen bonded peptide bonds that are likely engaged in weak intra-molecular hydrogen bonding as part of a local β-turn conformation.[47] The weakly hydrogen bonded β-turn is likely protected against amide-water

hydrogen bonds by the bulky β-branched side chains of Val, which are known to shield the peptide backbone from water molecules.[75] The absence of some peptide-water hydrogen bonds in the extended conformation of elastin as compared to typical unfolded peptides such as the XAO peptide which predominantly adopts a PPII conformation,[71,89–91] reduces the enthalpic advantage of the elastin's extended state over its entropically unfavorable collapsed state and narrows the free energy gap between the extended and collapsed states such that a temperature increase induces the inverse transition.

A lack of significant change in the AmI region at high temperature suggests the inverse temperature transition of elastin does not significantly impact the hydrogen bonding state of the peptide backbone. Furthermore, small intensity changes in the AmIII and $C_\alpha H_b$ band region indicate that elastin's phase transition is accompanied by only a small conformation change resulting in increased β-turn population. The increased β-turn content does not appear to impact the hydrogen bonding state of elastin. It is likely that the phase transition in elastin peptides is primarily driven by changes in conformation and/or hydration of the alkyl side chains.

Acknowledgments

The authors would like to thank Prof. D. W. Urry and Konstantin V. Pimenov for helpful discussions and NIH grant RO1 EB002053 for financial support.

REFERENCES

1. Alonso M, Reboto V, Guiscardo L, San Martin A, Rodriguez-Cabello JC. Macromolecules. 2000; 33:9480–9482.
2. Urry DW, Parker TM. Journal of Muscle Research and Cell Motility. 2002; 23:543–559. [PubMed: 12785104]
3. Li B, Alonso DOV, Bennion BJ, Daggett V. Journal of the American Chemical Society. 2001; 123:11991–11998. [PubMed: 11724607]
4. Li B, Alonso DOV, Daggett V. Journal of Molecular Biology. 2001; 305:581–592. [PubMed: 11152614]
5. Debelle L, Alix AJP, Wei SM, Jacob M-P. Eur J Biochem. 1998; 258:533–539. [PubMed: 9874220]
6. Fernandes RJ, Eyre DR. Biochemical and Biophysical Research Communications. 1999; 261:635–640. [PubMed: 10441478]
7. Herrera B, Eisenberg G, Holberndt O, Desco MM, Rábano A, García-Barreno P, Del Cañizo JF. Cryobiology. 2000; 41:43–50. [PubMed: 11017760]
8. Kim B-S, Nikolovski J, Bonadio J, Smiley E, Mooney DJ. Experimental Cell Research. 1999; 251:318–328. [PubMed: 10471317]
9. Lapis K, Tímár J. seminar in Cancer Biology. 2002; 12:209–217.
10. Lindholt JS, Heickendorff L, Vammen S, Fasting H, Henneberg EW. Eur J Vasc Endovasc Surg. 2001; 21:235–240. [PubMed: 11352682]
11. Nakamura F, Suyama K. Archives of Biochemistry and Biophysics. 1996; 325:167–173. [PubMed: 8561494]
12. Reiersen H, Rees AR. Biochemical and Biophysical Research Communications. 2000; 276:899–904. [PubMed: 11027566]
13. Robert L. seminar in Cancer Biology. 2002; 12:157–163.
14. Krukau A, Brovchenko I, Geiger A. Biomacromolecules. 2007; 8:2196–2202. [PubMed: 17567170]

15. Tamura T, Yamaoka T, Kunugi S, Panitch A, Tirrell DA. Biomacromolecules. 2000; 1:552–555. [PubMed: 11710180]
16. Bressan G, Prockop DJ. Biochemistry. 1977; 16:1406–1412. [PubMed: 557339]
17. Khaled MA, Prasad KU, Venkatachalam CM, Urry DW. Journal of the American Chemical Society. 1985; 107:7139–7145.
18. Urry DW, Chang DK, Krishna NR, Huang DH, Trapane TL, Prasad KU. Biopolymers. 1989; 28:819–833. [PubMed: 2720125]
19. Urry DW, Harris RD, Prasad KU. Journal of the American Chemical Society. 1988; 110:3303–3305.
20. Urry DW, Haynes B, Zhang H, Harris RD, Prasad KU. Proc Natl Acad Sci USA. 1988; 85:3407–3411. [PubMed: 2897120]
21. Urry DW, Peng S, Parker T. Journal of the American Chemical Society. 1993; 115:7509–7510.
22. Venkatachalam CM, Khaled MA, Sugano H, Urry DW. Journal of the American Chemical Society. 1981; 103:2372–2379.
23. Venkatachalam CM, Urry DW. Macromolecules. 1981; 14:1225–1229.
24. Urry DW. J Phys Chem B. 1997; 101:11007–11028.
25. Urry DW, Peng S, Xu J, McPherson DT. Journal of the American Chemical Society. 1997; 119:1161–1162.
26. Bressan G, Prockop DJ. Biochemisty. 1977; 16:1406–1412.
27. Debord SB, Lyon LA. J Phys Chem B. 2003; 107:2927–2932.
28. Ding Y, Ye X, Zhang G. Macromolecules. 2005; 38:904–908.
29. Reese CE, Mikhonin AV, Kamenjicki M, Tikhonov A, Asher SA. J Am Chem Soc. 2004; 126:1493–1496. [PubMed: 14759207]
30. Wang J, Gan D, Lyon LA, El-Sayed MA. J Am Chem Soc. 2001; 123:11284–11289. [PubMed: 11697971]
31. Wang X, Wu C. Macromolecules. 1999; 32:4299–4301.
32. Hoare T, Pelton R. Langmuir. 2004; 20:2123–2133. [PubMed: 15835661]
33. Hu T, You Y, Pan C, Wu C. J Phys Chem B. 2002; 106:6659–6662.
34. Jones CD, Lyon LA. Macromolecules. 2003; 36:1988–1993.
35. Kunugi S, Kameyama K, Tada T, Tanaka N, Shibayama M, Akashi M. Brazilian Journal of Medical and Biological Research. 2005; 38:1233–1238. [PubMed: 16082464]
36. Li C, Bergbreiter DE. Chemical Industries (Dekker). 2003; 89:545–550.
37. Zhu PW, Napper DH. Journal of Colloid and Interface Science. 1996; 177:343–352.
38. Zhu PW, Napper DH. J Phys Chem B. 1997; 101:3155–3160.
39. Zhu PW, Napper DH. Physical Review E: Statistical Physics, Plasmas, Fluids, and Related Interdisciplinary Topics. 2000; 61:6866–6871.
40. Reiersen H, Clarke AR, Rees AR. J Mol Biol. 1998; 283:255–264. [PubMed: 9761688]
41. Luan CH, Parker TM, Gowda DC, Urry DW. Biopolymers. 1992; 32:1251–1261. [PubMed: 1420992]
42. Frank HS. Journal of Chemcial Physics. 1945; 13:478–492.
43. Searle MS, Williams DH. J Am Chem Soc. 1992; 114:10690–10697.
44. Searle MS, Williams DH, Gerhard U. J Am Chem Soc. 1992; 114:10697–10704.
45. Tanford, C. The hydrophobic effect: formation of micelles and biological membranes. New York: Wiley; 1973.
46. Chang DK, Venkatachalam CM, Prasad KU, Urry DW. Journal of Biomolecular Structure & Dynamics. 1989; 6:851–858. [PubMed: 2590505]
47. Thomas GJ Jr, Prescott B, Urry DW. Biopolymers. 1987; 26:921–934. [PubMed: 3607249]
48. Gosline JM. Biopolymers. 1978; 17:697–707. [PubMed: 638231]
49. Gosline JM, French CJ. Biopolymers. 1979; 18:2091–2103. [PubMed: 497355]
50. Gosline JM, Yew FF, Weis-Fogh T. Biopolymers. 1975; 14:1811–1826.
51. Hoeve CAJ, Flory PJ. Biopolymers. 1974; 13:677–686. [PubMed: 4847581]

52. Bykov SB, Lednev IK, Ianoul A, Mikhonin AV, Asher SA. Appl Spectrosc. 2005; 59:1541–1552. [PubMed: 16390595]
53. Manning MC, Woody RW. Biopolymers. 1991; 31:569–586. [PubMed: 1868170]
54. Ahmed Z, Asher SA. Biochemistry. 2006; 45:9068–9073. [PubMed: 16866352]
55. Biron Z, Khare S, Samson AO, Hayek Y, Naider f, Anglister J. Biochemistry. 2002; 41:12687–12696. [PubMed: 12379111]
56. Foster JA, Bruenger E, Rubin L, Imberman M, Kagan H, Mecham R, Franzblau C. Biopolymers. 1975; 15:833–844.
57. Tamburro AM, Guantieri V, Daga-Gordini D, Abatangelo G. J Biol Chem. 1978; 253:2893–2894. [PubMed: 641043]
58. Dorman DE, Torchia DA, Bovey FA. Macromolecules. 1973; 6:80–82. [PubMed: 4778412]
59. Garrett, RHG., Charles, M. Biochemistry. Philadelphia, Pa: Saunders College Publishing; 1999.
60. Caswell DS, Spiro TG. J Am Chem Soc. 1987; 109:2796–2800.
61. Ahmed Z, Myshakina NS, Asher SA. manuscript in publication. 2007
62. Takeuchi H, Harada I. Journal of Raman Spectroscopy. 1990; 21:509–515.
63. Jordan T, Mukerji I, Wang Y, Spiro TG. J Mol Struct. 1996; 379:51–64.
64. Chen XG, Li P, Holtz JSW, Chi Z, Pajcini V, Asher SA, Kelly LA. J Am Chem Soc. 1996; 118:9716–9726.
65. Pajcini V, Asher SA. J Am Chem Soc. 1999; 121:10942–10954.
66. Asher SA, Ianoul A, Mix G, Boyden MN, Karnoup A, Diem M, Schweitzer-Stenner R. J Am Chem Soc. 2001; 123:11775–11781. [PubMed: 11716734]
67. Asher SA, Ianoul A, Mix G, Boyden MN, Karnoup A, Diem M, Schweitzer-Stenner R. J Am Chem Soc. 2001; 123:11775–11781. [PubMed: 11716734]
68. Lazarev YA, Grishkovsky BA, Khromova TB. Biopolymers. 1985; 24:1449–1478. [PubMed: 4041546]
69. Li P, Chen XG, Shulin E, Asher SA. J Am Chem Soc. 1997; 119:1116–1120.
70. Chi Z, Chen XG, Holtz JSW, Asher SA. Biochemistry. 1998; 37:2854–2864. [PubMed: 9485436]
71. Mikhonin AV, Ahmed Z, Ianoul A, Asher SA. J Phys Chem B. 2004; 108:19020–19028.
72. JiJi RD, Balakrishnan G, Hu Y, Spiro TG. Biochemistry. 2006; 45:34–41. [PubMed: 16388578]
73. Chourpa I, Ducel V, Richard J, Dubois P, Boury F. Biomacromolecules. 2006; 7:2616–2623. [PubMed: 16961325]
74. Cook WJ, Einspahr H, Trapane TL, Urry DW, Bugg CE. J Am Chem Soc. 1980; 102:5502–5505.
75. Avbelj F, Baldwin RL. Proc Natl Acad Sci USA. 2003; 100:5742–5747. [PubMed: 12709596]
76. Jordon T, Mukerji I, Yang W, Spiro TG. J Biol Chem. 1996; 379:51–64.
77. Wang Y, Purrello R, Jordan T, Spiro TG. J Am Chem Soc. 1991; 113:6359–6368.
78. Mikhonin AV, Ahmed Z, Ianoul A, Asher SA. J Phys Chem B. 2004; 108:19020–19028.
79. Lee S-H, Krimm S. Biopolymers. 1998; 46:283–317.
80. Overman SA, Thomas GJ Jr. Biochemistry. 1995; 34:5440–5451. [PubMed: 7727402]
81. Overman SA, Thomas GJ Jr. Biochemistry. 1998; 37:5654–5665. [PubMed: 9548951]
82. Overman SA, Thomas GJ Jr. J Raman Spectrosc. 1998; 29:23–29.
83. Mikhonin AV, Bykov SV, Myshakina NS, Asher SA. J Phys Chem B. 2006; 110:5509–5518.
84. Mikhonin AV, Asher SA. J Phys Chem B. 2005; 109:3047–3052. [PubMed: 16851319]
85. Ahmed Z, Illir AB, Mikhonin AV, Asher SA. J Am Chem soc. 2005; 127:10943–10950. [PubMed: 16076200]
86. Lednev IK, Karnoup AS, Sparrow MC, Asher SA. J Am Chem Soc. 1999; 121:8074–8086.
87. Perry A, Stypa MP, Foster JA, Kumashiro KK. J Am Chem Soc. 2002; 124:6832–6833. [PubMed: 12059197]
88. Ohgo K, Ashida J, Kumashiro KK, Asakura T. Macromolecules. 2005; 38:6038–6047.
89. Shi Z, Olson CA, Rose GD, Baldwin RL, Kallenbach NR. Proc Natl Acad Sci USA. 2002; 99:9190–9195. [PubMed: 12091708]

90. Schweitzer-Stenner R, Eker F, Griebenow K, Cao X, Nafie LA. J Am Chem Soc. 2004; 126:2768–2776. [PubMed: 14995194]

91. Stapley BJ, Creamer TP. Protein Sci. 1999; 8:587–595. [PubMed: 10091661]

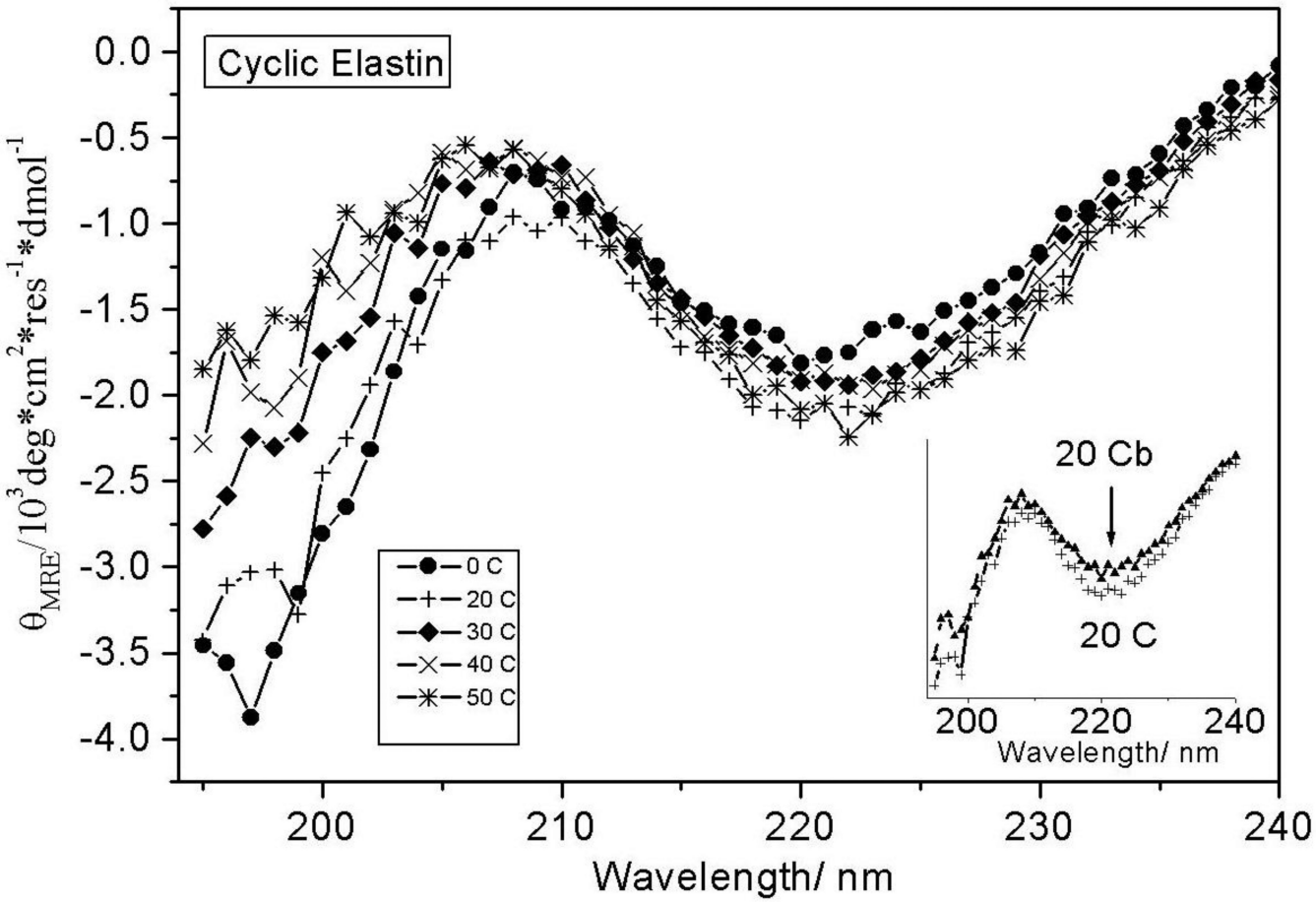

Figure 1.

Temperature dependent CD spectra of cyclic elastin. The insert shows the 20 °C CD spectra of cyclic elastin during and subsequent to heating. The CD spectrum subsequent to heating (20 °Cb) shows a slight overall decrease in spectral intensity after heating. This change likely derives from temperature induced degassing/bubble formation on cell walls at high temperatures.

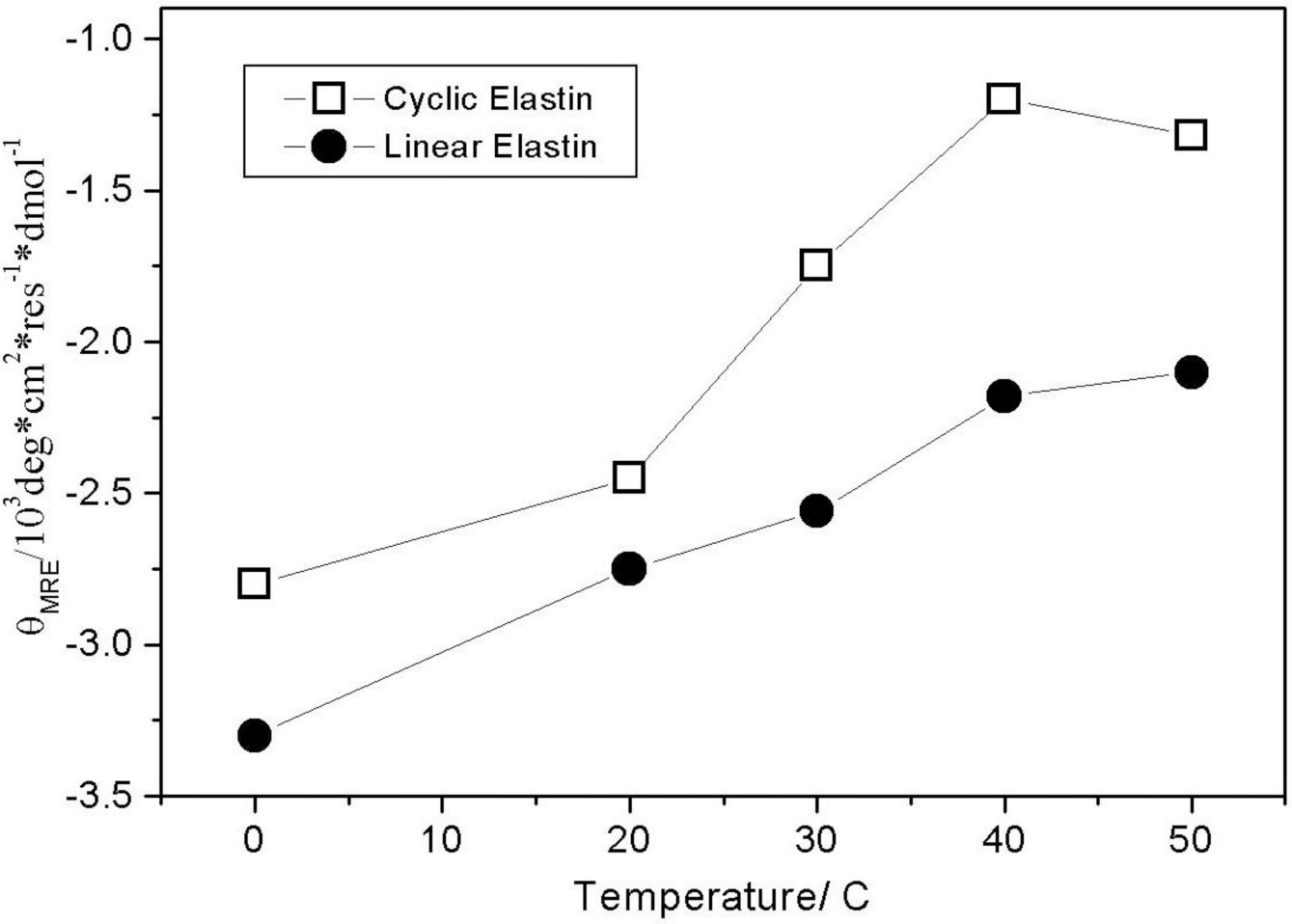

Figure 2.
Temperature dependent changes in the mean residue ellipticities of cyclic and linear elastin at 200 nm.

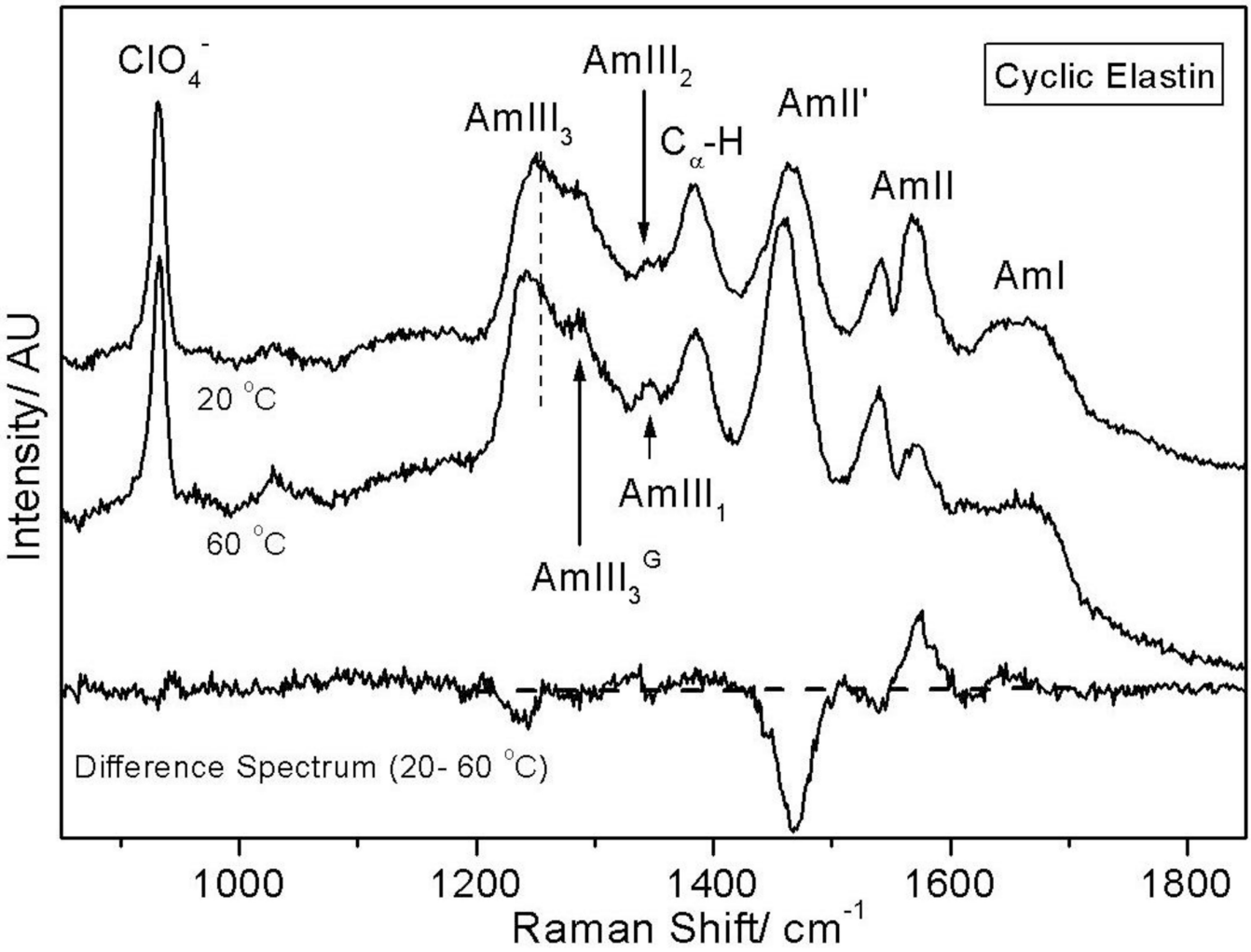

Figure 3.

204 nm UV resonance Raman spectra of cyclic elastin measured at 20 and 60 °C normalized to the intensity of 932 cm^{-1} perchlorate band. The difference spectrum shows temperature dependent changes in the conformation-sensitive $AmIII_3$ region, as well as intensity changes in the C_α-H_b. The AmII'p narrows at 60 °C suggesting the proline peptide bonds adopt a more well-defined conformation at higher temperatures. The trough in the AmII region is an artifact that derives from over-subtraction of the interfering O_2 stretching vibration at 1560 cm^{-1} when the NMR tube contribution was subtracted from the measured spectra.

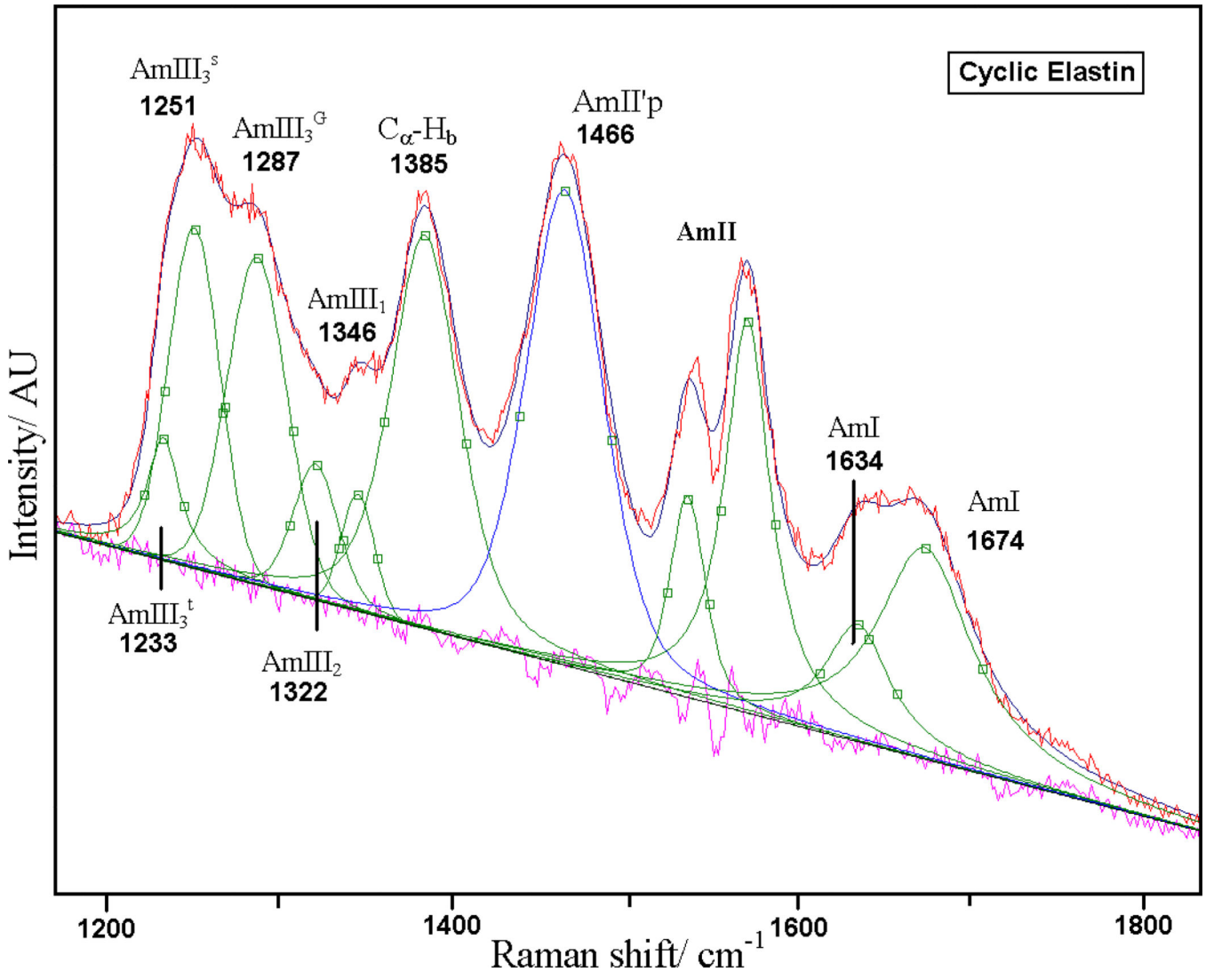

Figure 4.

Spectral deconvolution of 20 °C 204 nm UV resonance Raman spectra of cyclic elastin with mixed Gaussian and Lorentzian bands. The quality of the fit is evident from the flat residual displayed underneath.

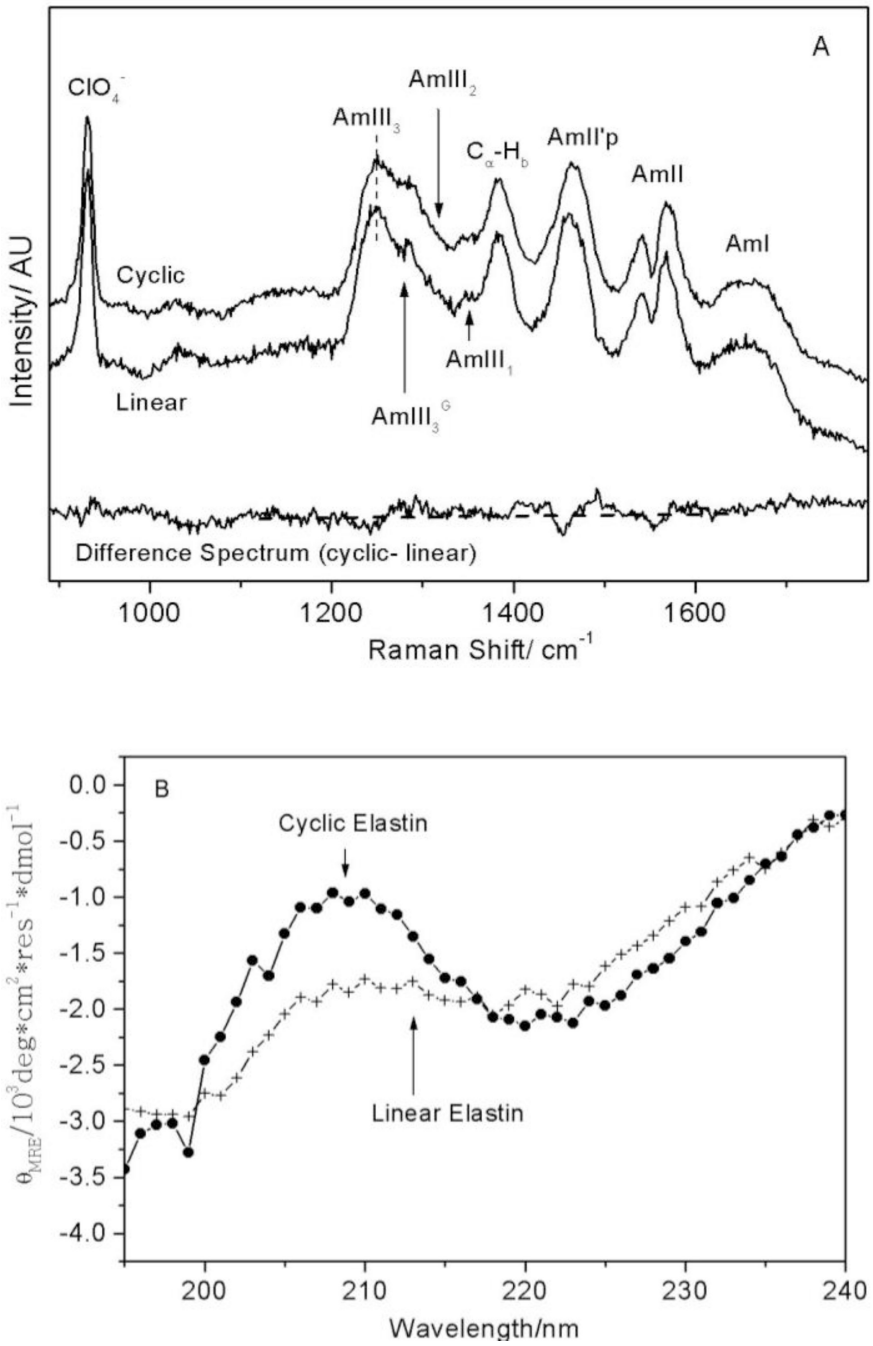

Figure 5.

A) 204 nm UV resonance Raman spectra of linear and cyclic elastin at 20 °C and their difference spectra. The featureless difference spectrum indicates that the Val and Pro peptide bonds in cyclic and linear peptides have similar conformations. B) CD spectra of linear and cyclic elastin at 20 °C. Cyclic elastin shows a more prominent positive feature at ~207 nm, indicating a greater population of β-type II turns in the cyclic peptide.

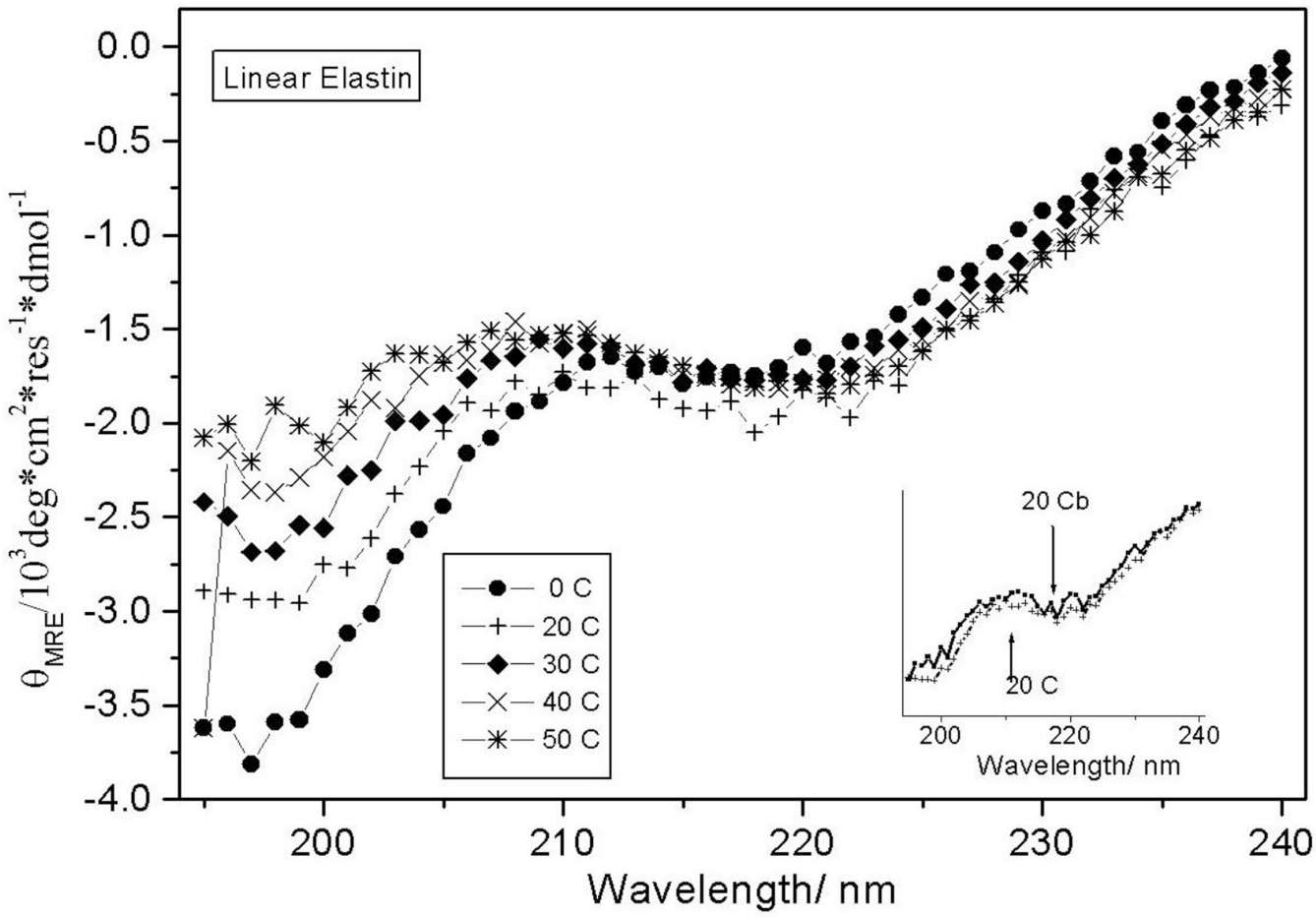

Figure 6.

Temperature dependent CD spectra of linear elastin. The insert shows the 20 °C CD spectra of cyclic elastin during and subsequent (20 °C) to heating.

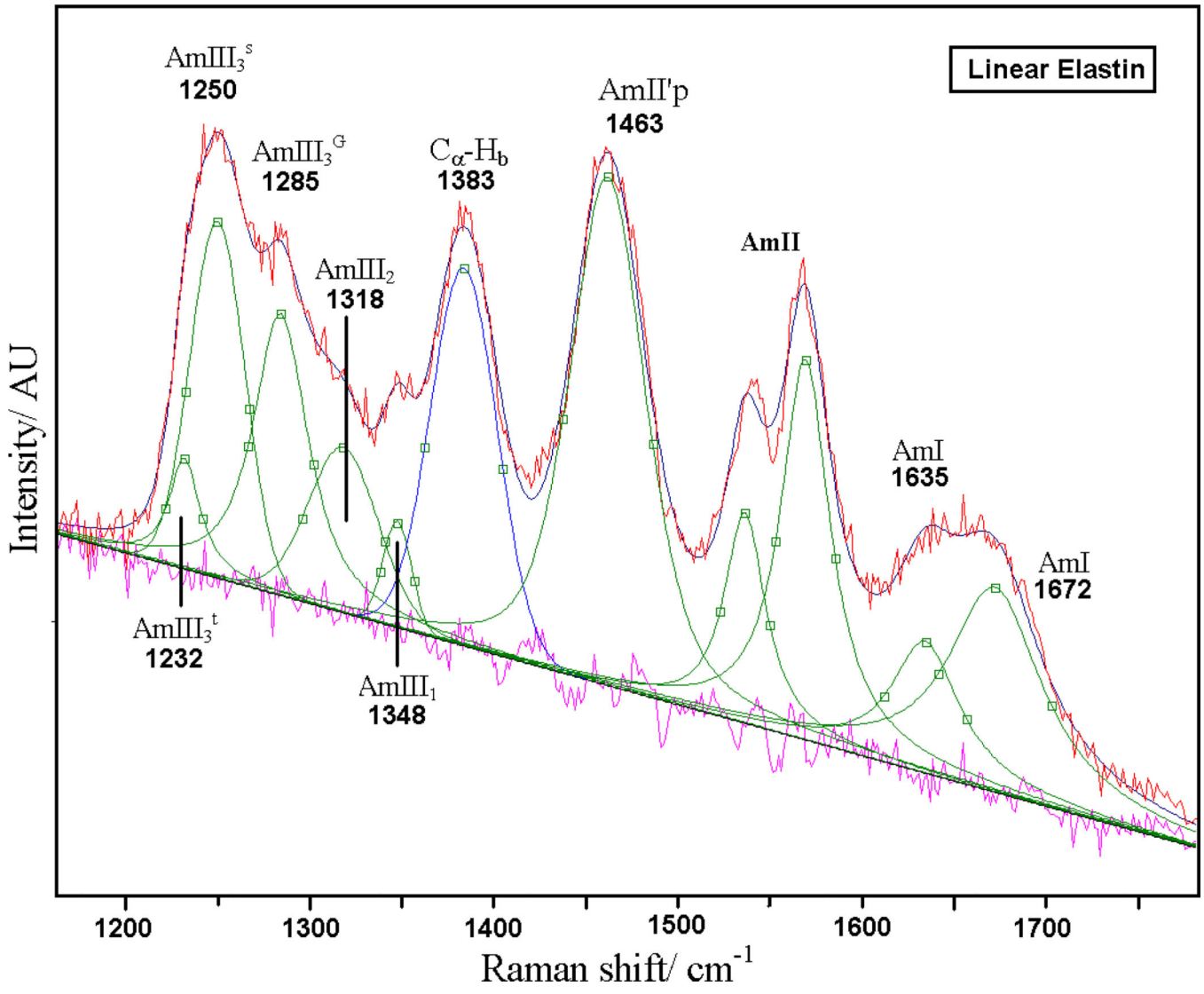

Figure 7.

Spectral deconvolution of 20 °C 204 nm UV resonance Raman spectra of linear elastin with Gaussian and Lorentzian bands. The quality of the fit is evident from the flat residual.

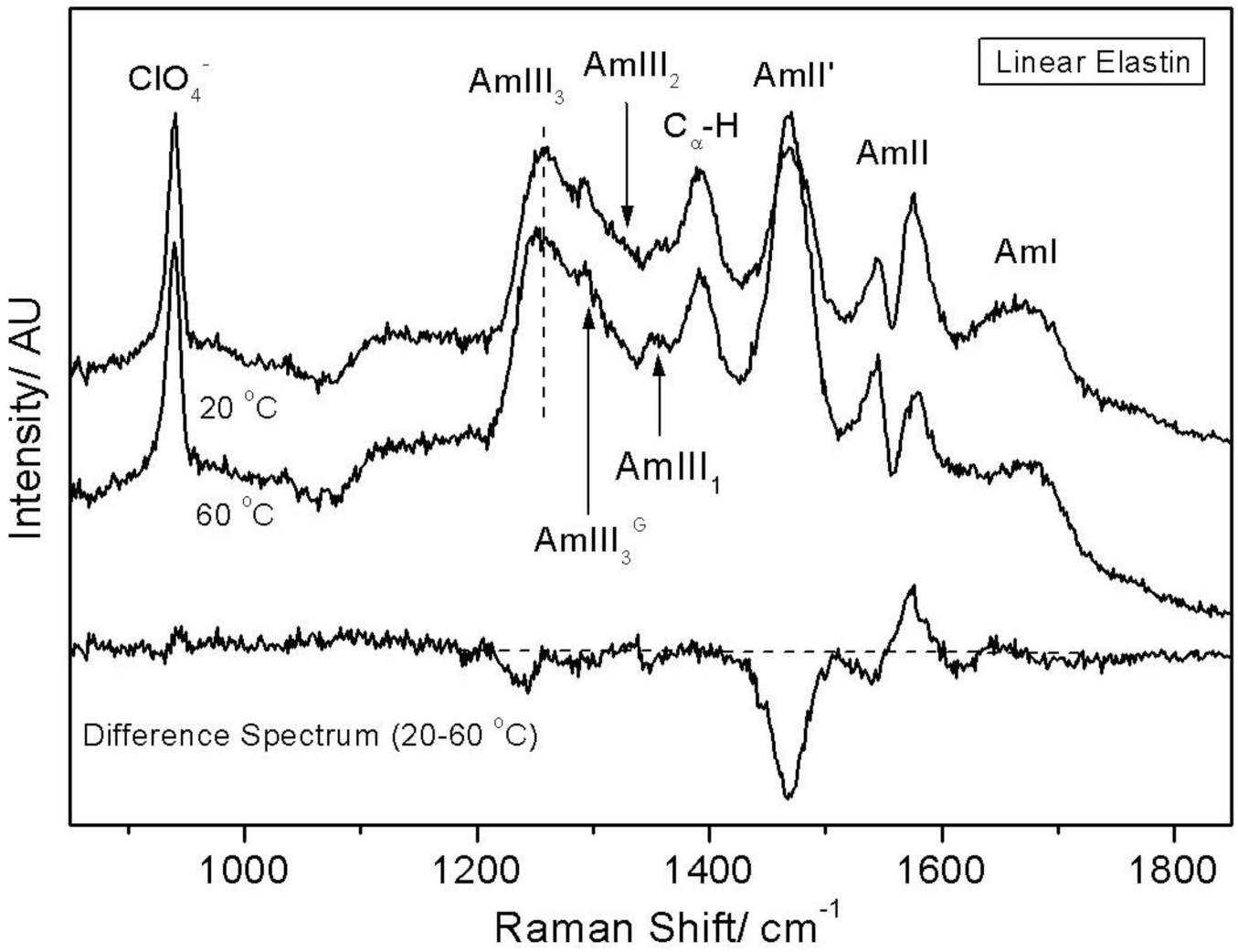

Figure 8.

204 nm UV resonance Raman spectra of linear elastin measured at 20 and 60 °C. The difference spectrum shows narrowing of the AmII' band width at 60 °C which is indicative of a transition to a relatively well-defined conformation. The trough in the AmII region is an artifact that derives from over-subtraction of the interfering O_2 stretching vibration at 1560 cm^{-1} when the NMR tube contribution was subtracted from the measured spectra.

Table 1

Conformation Distribution of Linear and Cyclic Elastin

Band Position (cm^{-1})	**Ψ Angle (degree)**	**Conformation**
Cyclic Elastin		
1251	−35°	β-Type III turn
	+165°	Distorted β-strand
1233	0°	β-Type II turn
Linear Elastin		
1250	−35°	β-Type III turn
	+165°	Distorted β-strand
1230	0°	β-Type II turn